International Journal of Pharmaceutics: X 6 (2023) 100193

Contents lists available at ScienceDirect

International Journal of Pharmaceutics: X

journal homepage: www.sciencedirect.com/journal/international-journal-of-pharmaceutics-x

Chicken embryo model for *in vivo* acute toxicological and antitumor efficacy evaluation of lipid nanocarrier containing doxorubicin

Aline de Cristo Soares Alves [a,*], Danieli Rosane Dallemole [a], Taiane Medeiro Ciocheta [a], Augusto Ferreira Weber [b], Samanta da Silva Gündel [a], Fernanda Visioli [c,d], Fabricio Figueiró [b], Silvia Stanisçuaski Guterres [a], Adriana Raffin Pohlmann [a]

[a] *Programa de Pós-Graduação em Ciências Farmacêuticas, Faculdade de Farmácia, Universidade Federal do Rio Grande do Sul, Av. Ipiranga, 2752, Porto Alegre, 90610-000, RS, Brazil*

[b] *Programa de Pós-Graduação em Ciências Biológicas: Bioquímica, Instituto de Ciências da Saúde, Universidade Federal do Rio Grande do Sul, Rua Ramiro Barcelos, 2600, Porto Alegre, RS 90035-003, Brazil*

[c] *Programa de Pós-Graduação em Odontologia, Faculdade de Odontologia, Universidade Federal do Rio Grande do Sul, Rua Ramiro Barcelos, 2492, Porto Alegre, RS 90035-003, Brazil*

[d] *Centro de Pesquisa Experimental, Hospital de Clínicas de Porto Alegre, Rua Ramiro Barcelos, 2350, Porto Alegre, RS 90035-903, Brazil*

ARTICLE INFO

Keywords:
Nanotechnology
Alternative animal model
CAM assay
Toxicity
Tumor
MCF-7 cell line

ABSTRACT

Nanoencapsulation of chemotherapeutics, including doxorubicin, can endow the formulations with unique properties, such as a decrease in adverse effects and toxicity. The chicken embryo model is an alternative and well-accepted strategy for evaluating the toxicity and efficacy of drugs and nanoformulations. Therefore, this study proposes the development of a new lipid nanocarrier for doxorubicin delivery (NanoLip-Dox) and posterior evaluation of toxicological profile and antitumoral efficacy against a breast tumor in chicken embryos. NanoLip-Dox showed a unimodal particle size (< 150 nm), negative zeta potential (−19.5 mV), absence of drug crystals, drug content of 0.099 mg·mL^{-1}, and high entrapment efficiency (95%). NanoLip-Dox did not cause toxicity in the chicken embryos; in contrast, doxorubicin hydrochloride induced moderate irritation in the chorioallantoic membrane (at 862.1 μmol·L^{-1}), a survival rate of 50% (at 1.7 μmol·L^{-1}), and an increase in aspartate aminotransferase (at 862.1, 344.8, and 172.4 μmol·L^{-1}). In addition, NanoLip-Dox (at 1.7 μmol·L^{-1}) showed potent antitumor efficacy with a high tumor remission percentage (40.9 ± 9.7%) compared to the control group (8.6 ± 14.8%). These findings together with the absence of toxicity concerning morphological characteristics, weights of embryos and organs, hematologic parameters, and enzymatic activity (alanine aminotransferase, aspartate aminotransferase, and creatinine) suggest the safety and efficacy of NanoLip-Dox.

1. Introduction

Toxicity and efficacy studies are essential for pharmaceutical development and production of new medications (Chen et al., 2021). In recent decades, models that fit the well-established 3Rs concept of animal experimentation have been investigated (Chapman et al., 2013). The 3Rs rule comprises the search for alternatives to replace or reduce the number of animals and refine assays to ensure minimum pain or stress to animals (Russell and Burch, 1959; Chen et al., 2021). The chicken embryo model is a well-accepted strategy for the replacement or refinement of the use of animal models (Kucinska et al., 2017). For over a century, this model has been employed in biological, pharmaceutical, and medical studies (Chen et al., 2021).

The biocompatibility and safety of new formulations can be evaluated by analyzing the parameters of the chorioallantoic membrane (CAM) or embryonic tissues (Huang et al., 2015; Moreno-Jiménez et al.,

Abbreviations: ALT, alanine aminotransferase; AST, aspartate aminotransferase; CAM, chorioallantoic membrane; D[4,3]v, volume-weighted mean diameter; D_h, hydrodynamic mean diameter determined by nanoparticle tracking analysis; Dox.HCl, doxorubicin hydrochloride; MCF-7, human breast adenocarcinoma; NanoLip, unloaded lipid nanocarrier; NanoLip-Dox, lipid nanocarrier containing doxorubicin; PDI, polydispersity index; PND, particle number density; Span, polydispersity; z-average d_h, hydrodynamic mean diameter determined by dynamic light scattering.

* Corresponding author.
E-mail address: alves.alinecs@yahoo.com.br (A. de Cristo Soares Alves).

https://doi.org/10.1016/j.ijpx.2023.100193

Available online 24 June 2023

2017). Formulations administered to the CAM can reach the systemic circulation and affect normal development of the embryo (Moreno-Jiménez et al., 2017; Ribatti, 2017). Furthermore, drugs or formulations administered to the CAM are metabolized and degraded, which can provide a predictive model for toxicity (Kue et al., 2015). Thus, some toxicological parameters can be evaluated, including direct effects on the CAM, embryo survival rate, morphological alterations, body weight, and damage to the vasculature or organs (Rampino et al., 2013; Rampino et al., 2016; Kurantowicz et al., 2017; Chen et al., 2021).

In addition, chicken embryos support the implantation of a variety of normal or tumor cells, organs, and tissues - including those of humans, – owing to the slow development of the immune system associated with a rich vascular supply (Murphy, 1914; Honda et al., 2015; Vu et al., 2018). After implantation of the tumor cells (2–5 days), the solid tumor rapidly develops, unlike the long period required for tumor development in mice or rats (3–6 weeks) (Ribatti and Tamma, 2018; Vu et al., 2018). Thus, this model has been widely used to study tumor cell invasion, angiogenesis, and metastasis (Lokman et al., 2012; Liu et al., 2013; Augustine et al., 2020).

The chicken embryo model has several advantages over animal models, including easy handling, low cost, and rapid development of embryos, allowing rapid acquisition of experimental results (Nowak-Sliwinska et al., 2014; Kundeková et al., 2021). Embryonic development is approximately achieved in 21 days (Hamburger–Hamilton stages) (Kurantowicz et al., 2017). In addition, the egg yolk serves as a nutrient source for embryos; thus, no culture medium is necessary to grow embryos until hatching (Huang et al., 2015).

Therefore, the chicken embryo model has been extensively used to evaluate the toxicity and efficacy of new nanoformulations (Blasi et al., 2013; Roman et al., 2013; Predoi et al., 2020). Drug nanoencapsulation endows the formulation with unique properties that can decrease its adverse effects and toxicity compared to those of the drug in solution, thereby enhancing the drug bioavailability and efficacy (Wilczewska et al., 2012; Schütz et al., 2013; Borišev et al., 2018; Fonseca et al., 2021). Doxorubicin is one of the most common chemotherapeutic agents used for the treatment of hematological and solid cancers, including breast cancer; however, adverse effects such as cardiotoxicity and hepatotoxicity have been reported (Al-Malky et al., 2020). Teratogenic and genotoxic effects have been reported in embryos of chicks, zebrafish, rats, and mice (Menegola et al., 2001; Aleksandar et al., 2019; Andersen et al., 2019; Abed et al., 2020). The mechanism of action is related to DNA intercalation, which causes the inhibition of DNA topoisomerase IIα, replication, and transcription processes, as well as the suppression of cellular functions and free radical generation (Shingadia, 2015; Borišev et al., 2018; Alavi and Nokhodchi, 2020; Al-Malky et al., 2020).

Doxorubicin nanoformulations have been used clinically (liposomes) and evaluated in clinical trials (liposomes, polymeric nanoparticles, and polymeric micelles, among others). Most formulations have several advantages over drug salts in solution, such as cardiotoxicity reduction (Barenholz, 2012); however, they can be further improved concerning drug loading, poor release at the tumor site (Toley et al., 2013; Zhao et al., 2013), and mucositis as site effect (Perez et al., 2002; Leonard et al., 2009). Thus, doxorubicin remains the subject of studies, searching for more efficient nanocarriers associated with low cytotoxicity.

In view of the above, this paper proposes the development of a new lipid nanocarrier with a globule consisting of caprylic/capric triglyceride, sorbitan monostearate (solid), sorbitan monooleate (liquid), and oleic acid. Oleic acid served as a counterion to electrostatically bind doxorubicin; lecithin and polysorbate 80 were used as surfactants to physically stabilize the globules dispersed in water. This formulation was designed to serve as a nanocarrier for the delivery and targeting of doxorubicin to solid tumors. In addition, we aimed to evaluate the safety and antitumor efficacy of the nanoformulation using the chicken embryos as an alternative animal model.

2. Material and methods

2.1. Materials

Sorbitan monostearate (Span 60®), sorbitan monooleate (Span® 80), doxorubicin hydrochloride (Dox.HCl, 98–102%), polysorbate 80 (Tween® 80), and trifluoroacetic acid were purchased from Sigma-Aldrich Co. (St. Louis, Missouri, USA). Caprylic/capric triglyceride and soybean lecithin (Lipoid S75®) were supplied by Delaware (Porto Alegre, Brazil) and Lipoid (Ludwigshafen, Germany), respectively. Oleic acid was obtained from Labsynth (Diadema, Brazil). Trypan blue and analytical-grade acetone were purchased from Neon (Suzano, Brazil). Analytical-grade ethanol and high-performance liquid chromatography-grade acetonitrile were obtained from Química Moderna (Barueri, Brazil) and Merck (Darmstadt, Germany), respectively.

2.2. Development of new lipid nanocarrier containing doxorubicin

The nanoformulation was produced *via* spontaneous emulsification. The organic phase consisted of sorbitan monostearate (0.02 g), caprylic/capric triglyceride (0.04 g), sorbitan monooleate (0.04 g), oleic acid (0.04 g), soybean lecithin (0.06 g), and Dox.HCl (1 mg) dissolved in ethanol (25 mL) and acetone (5 mL) with magnetic stirring at 40 °C. The aqueous phase consisted of polysorbate 80 (80 mg) and ultrapure water (50 mL). After complete solubilization of all the components, the organic phase was poured into the aqueous phase with stirring for 10 min. The organic solvent was removed, and the resultant translucent solution was concentrated under reduced pressure (Rotavapor® RII, Büchi, Switzerland) at 40 °C until a final volume of 9 mL. Subsequently, the volume was adjusted to 10 mL by adding ultrapure water. The final formulation, named NanoLip-Dox, had a theoretical doxorubicin content of 0.1 $mg{\cdot}mL^{-1}$. A blank formulation without the drug was also prepared as described above and was named NanoLip.

2.3. Physicochemical characterization of nanoformulations

NanoLip and NanoLip-Dox were physicochemically characterized, and all results are expressed as the mean ± standard deviation determined from three independent batches of each formulation.

Each nanoformulation was evaluated by laser diffraction (Mastersizer 2000 Instrument, Malvern, UK) to determine the size distribution in the range of 40 nm – 2 mm using the Mie theory to calculate the diameter distribution curves, volume-weighted mean diameter (D[4,3] v) and polydispersity (Span). The dispersion unit (Hydro 2000SM-AWM2002, Malvern, UK) was filled with distilled water and stirred at 2000 rpm, and each sample was then applied drop-wise into the wet unit until an obscuration of 2% was reached.

The size distribution was evaluated by dynamic light scattering (Zetasizer Nano-ZS Instrument, Malvern, UK) to determine the diameters of the populations between 1 nm and 2000 nm. Mono-exponential fitting of the size distribution curve (method of Cumulants) was conducted to calculate the hydrodynamic mean diameter (z-average d_h) based on the intensity of the scattered light. The polydispersity index (PDI) was calculated as the square of the standard deviation (distribution curve) divided by the square of the mean diameter. The samples were diluted (1:500, v/v) in ultrapure water and analyzed using a 633-nm red laser at 25 °C.

Each nanoformulation was also evaluated by nanoparticle tracking analysis (NanoSight LM10 Instruments, NanoSight Ltd., Salisbury, UK). The size distribution curve was determined, and the mean hydrodynamic diameter (by the number of particles) and particle number density (PND) were calculated. The samples were diluted (1:10,000, v/v) in ultrapure water and analyzed using a 638-nm red laser. A video was recorded for 60 s for each sample and processed using the NTA 3.2 analytical software.

Zeta potential was determined by measuring electrophoretic

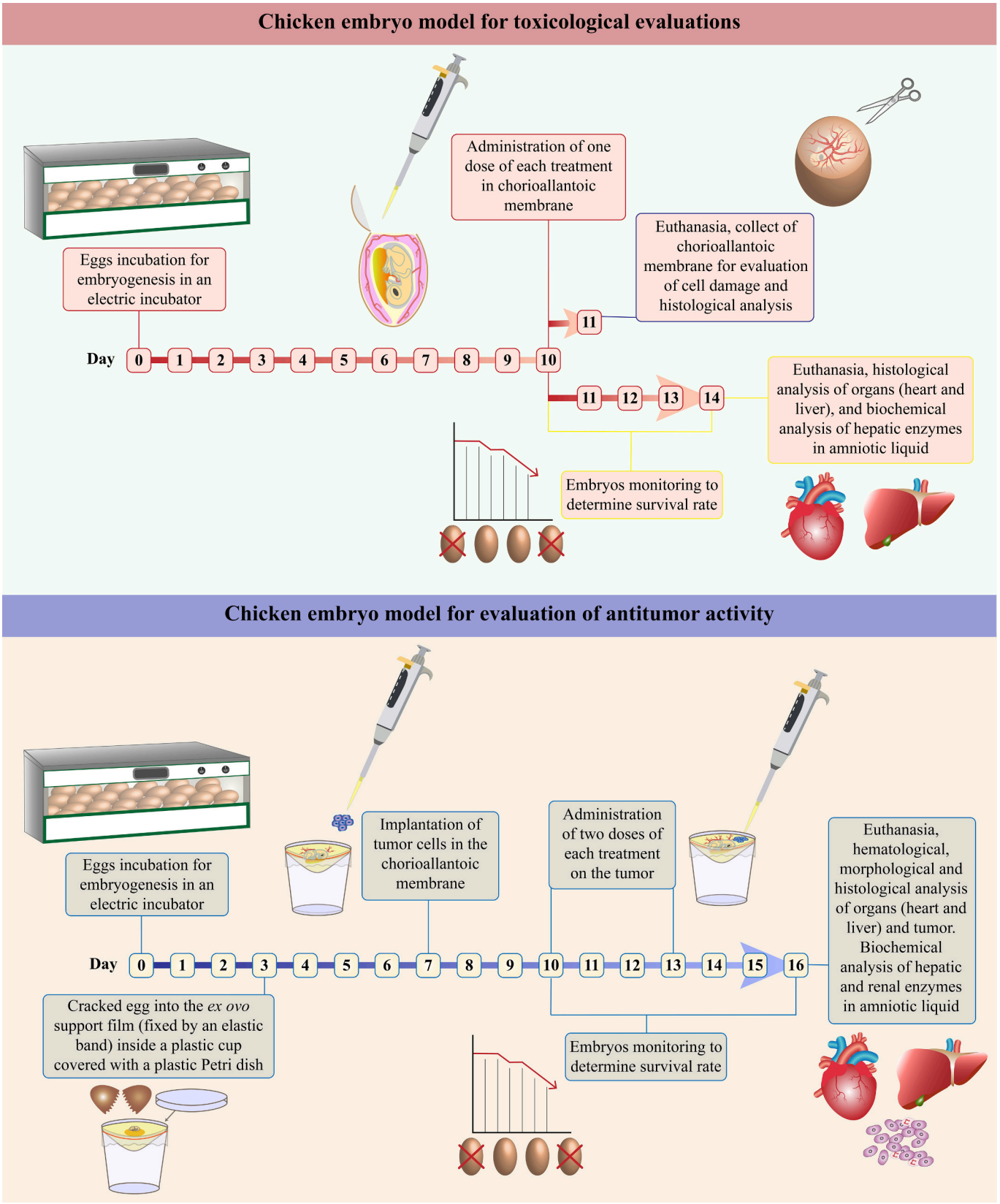

Fig. 1. Experimental design of chicken embryo model for toxicological and antitumor activity evaluations.

Table 1
Physicochemical characterization of NanoLip and NanoLip-Dox.

Parameter	NanoLip	NanoLip-Dox
D[4,3]v (nm)	132 ± 2 [a]	137 ± 2 [a]
Span	0.9 ± 0.0 [a]	1.1 ± 0.1 [b]
z-average d_h (nm)	117 ± 5 [a]	144 ± 16 [b]
PDI	0.2 ± 0.0 [a]	0.2 ± 0.0 [a]
Zeta potential (mV)	−15.5 ± 1.3 [a]	−19.5 ± 2.5 [a]
D_h (nm)	160 ± 3 [a]	190 ± 2 [b]
PND (globules·mL^{-1})	(6.2 ± 1.4) × 10^{12} [a]	(3.0 ± 2.5) × 10^{12} [a]
Drug content (mg·mL^{-1})	–	0.099 ± 0.2
Entrapment efficiency (%)	–	95.3 ± 2.6

NanoLip, unloaded lipid nanocarrier; NanoLip-Dox, lipid nanocarrier containing doxorubicin; D[4,3]v, volume-weighted mean diameter; Span, polydispersity; z-average d_h, hydrodynamic mean diameter determined by dynamic light scattering; PDI, polydispersity index; D_h, hydrodynamic mean diameter determined by nanoparticle tracking analysis; PND, particle number density.
[a,b] Mean ± standard deviation ($n = 3$) analyzed per line, where different letters represent statistical differences (Student's *t*-test, $p < 0.05$).

mobility using laser Doppler velocimetry (Zetasizer Nano-ZS instrument, Malvern, UK). The samples were diluted (1:500, v/v) in a 10 mmol·L^{-1} aqueous sodium chloride solution to guarantee the minimum conductivity required for analysis.

Nanoformulations were analyzed by transmission electron microscopy using a JEOL JEM-1011 instrument (JEOL Company, Tokyo, Japan) operating at 100 kV. Samples diluted in water (1:10, v/v) were deposited on the 400 mesh copper grids (10 µL) and stained with uranyl acetate solution (10 µL, 2% w/v).

The drug content (direct quantitative content analysis) and entrapment efficiency (indirect quantitative content analysis) of doxorubicin in NanoLip-Dox were determined by liquid chromatography (HPLC Shimadzu equipment comprising a CBM-20A controller, an SPD-M20AV detector, an LC-20AT pump, and an SIL-20A auto-sampler, Japan) using a previously validated method (Antonow et al., 2017). The chromatographic conditions were as follows: C18 column (150 mm × 4.6 mm × 5 µm, Waters), mobile phase in aqueous trifluoroacetic acid (0.01%, v/v) and acetonitrile (50:50, v/v) solutions at an apparent pH of 2.6, flow rate of 1 mL·min^{-1}, injection volume of 50 µL, and wavelength of 254 nm. To determine the drug content (C_{total}), the formulation (250 µL) was poured into a volumetric flask (5 mL) containing the mobile phase with magnetic stirring for 20 min and subsequently analyzed by HPLC. The entrapment efficiency was determined using the ultrafiltration–centrifugation technique. An aliquot (400 µL) was added to an ultrafilter (Amicon® Merck Millipore, 10 kDa) and centrifuged for 10 min at 1844 ×*g*. The ultrafiltrate was injected (without dilution) for quantification ($C_{ultrafiltrate}$). The entrapment efficiency (in percentage) of doxorubicin was calculated using Eq. (1).

$$EE\ (\%) = \frac{C_{Total} - C_{Ultrafiltate}}{C_{Total}} \times 100 \quad (1)$$

The *in vitro* release profiles of NanoLip-Dox and free drug were determined in artificial biomimetic environment using dialysis membrane (cutoff 14,000 Da) as previously determined by Cé et al. (2016) with modifications. Release medium consisted of phosphate buffer saline (PBS, pH 7.4). Samples of free drug and nanoformulation were prepared at 50 and 100 µg·mL^{-1} Dox.HCl, respectively. Free drug was dispersed in the release medium. Samples (2 mL) were added into dialysis membrane and immersed in release medium (50 mL) under moderate stirring at 37 °C for 48 h following the *sink* conditions. At predetermined times (0.5, 1, 2, 3, 6, 9, 12, 24 and 48 h), a sample (1.5 mL) was withdrawn and the released drug content was quantified by HPLC. The kinetic analyses of data were performed using the mathematics models, such as zero order, first order, second order, Higuchi and Korsmeyer–Peppas calculated by Scientist® 2.0 software (MicroMath®, USA). Best-fitted model was considered with higher model selection criteria (MSC) and correlation coefficient (r) values.

2.4. Experiments with chicken embryo model

All experiments were approved by the Local Animal Ethical Committee of the Universidade Federal do Rio Grande do Sul (protocols #36922 and #410471). Undeveloped fertilized chicken eggs (*Gallus gallus*) were supplied by the Aviário de Ensino e Pesquisa do Departamento de Zootecnia, Universidade Federal do Rio Grande do Sul (UFRGS). The eggs were disinfected with 70% ethanol and incubated for embryogenesis in an electric incubator (ChocMais, Brazil) at 37.5 °C with automatic rotation once per hour. For subsequent experiments, the eggs were randomly divided into different groups. At the end of each experiment, embryos were euthanized by decapitation.

2.4.1. Chicken embryo model for toxicological evaluations

The toxicological assays consisted of CAM ($n = 7$) and embryotoxicity ($n = 8$) evaluations. On embryo development day 10, the eggs were opened with forceps on the air chamber side, and the CAM was exposed by removing the shell membrane. The treatments were diluted in 0.9% saline solution to reach a final volume of 100 µL, and one dose was administered to the CAM. Subsequently, the eggs were sealed with parafilm and incubated in a climatic chamber (Nova Ética 420-CLD, Brazil) at 80% relative humidity and 37.5 °C for additional 24 h (CAM assay) or 96 h (embryotoxicity assay). The experimental design of the chicken embryo model used for the toxicological evaluation is shown in Fig. 1.

2.4.1.1. Evaluation of inflammatory response and cell damage in CAM.

The groups consisted of control (0.9% saline solution), NaOH (0.1 mol·L^{-1} aqueous sodium hydroxide solution), Dox.HCl in solution (862.1, 344.8, 172.4, 34.5, and 1.7 µmol·L^{-1}), and NanoLip-Dox (containing 172.4, 86.2, 34.5, 1.7, and 0.2 µmol·L^{-1} of Dox.HCl).

After 24 h of treatment (embryo development day 11), the CAM was removed and completely cleaned with saline solution ($n = 3$). The membranes were immediately fixed in 10% phosphate-buffered formalin (pH 7.4) for 24 h, dehydrated in a series of ethanol solutions, cleared with xylol, and infiltrated in paraffin. Paraffin blocks were cut into sections of 5 µm for hematoxylin and eosin staining. The stained slides were observed under an optical microscope (Eclipse Si Microscope, Nikon, United States) to evaluate inflammation and tissue responses. Inflammation was scored for inflammatory infiltrate, hyperemia, and hemorrhage on a scale of 0–3 depending on their intensity (0, absence; 1, mild; 2, moderate; 3, intense). The results are expressed as the mean ± standard deviation ($n = 3$).

The degree of CAM injury was assessed after 24 h of treatment ($n = 4$) based on the amount of trypan blue absorbed (nmol·mL^{-1}). Trypan blue solution (0.5 mL, 0.1%, m/v) was added to the CAM for 1 min. The excess dye was cleaned with saline solution, and the CAM was removed. Trypan blue absorbed by the CAM was extracted with 1 mL formamide for 24 h and subsequently analyzed using a spectrophotometer at 595 nm (UV-1800PC, Pró-Análise, Brazil). A calibration curve of trypan blue was drawn, and a linear equation was obtained (0.1–57.3 nmol·mL^{-1}). Samples that showed values lower than 7.0 nmol·mL^{-1}, between 7.0 and 14.5 nmol·mL^{-1}, and higher than 14.5 nmol·mL^{-1} were classified as non- or weak, moderate, and severe irritants, respectively (Lagarto et al., 2006).

2.4.1.2. Determination of survival rate, hepatoxicity, and cardiotoxicity.

The groups consisted of control (0.9% saline solution), Dox.HCl solution (862.1, 344.8, 172.4, 34.5, and 1.7 µmol·L^{-1}), and NanoLip-Dox (containing 172.4, 86.2, 34.5, 1.7, and 0.2 µmol·L^{-1} of Dox.HCl).

Embryos were monitored daily until embryo development day 14 (96 h after treatment) to verify the mortality ($n = 8$). The embryo survival rate was calculated as the percentage of survived embryos and the survival curves were constructed. At the end of the experiment, the amniotic fluids were collected, embryos were euthanized, and organs

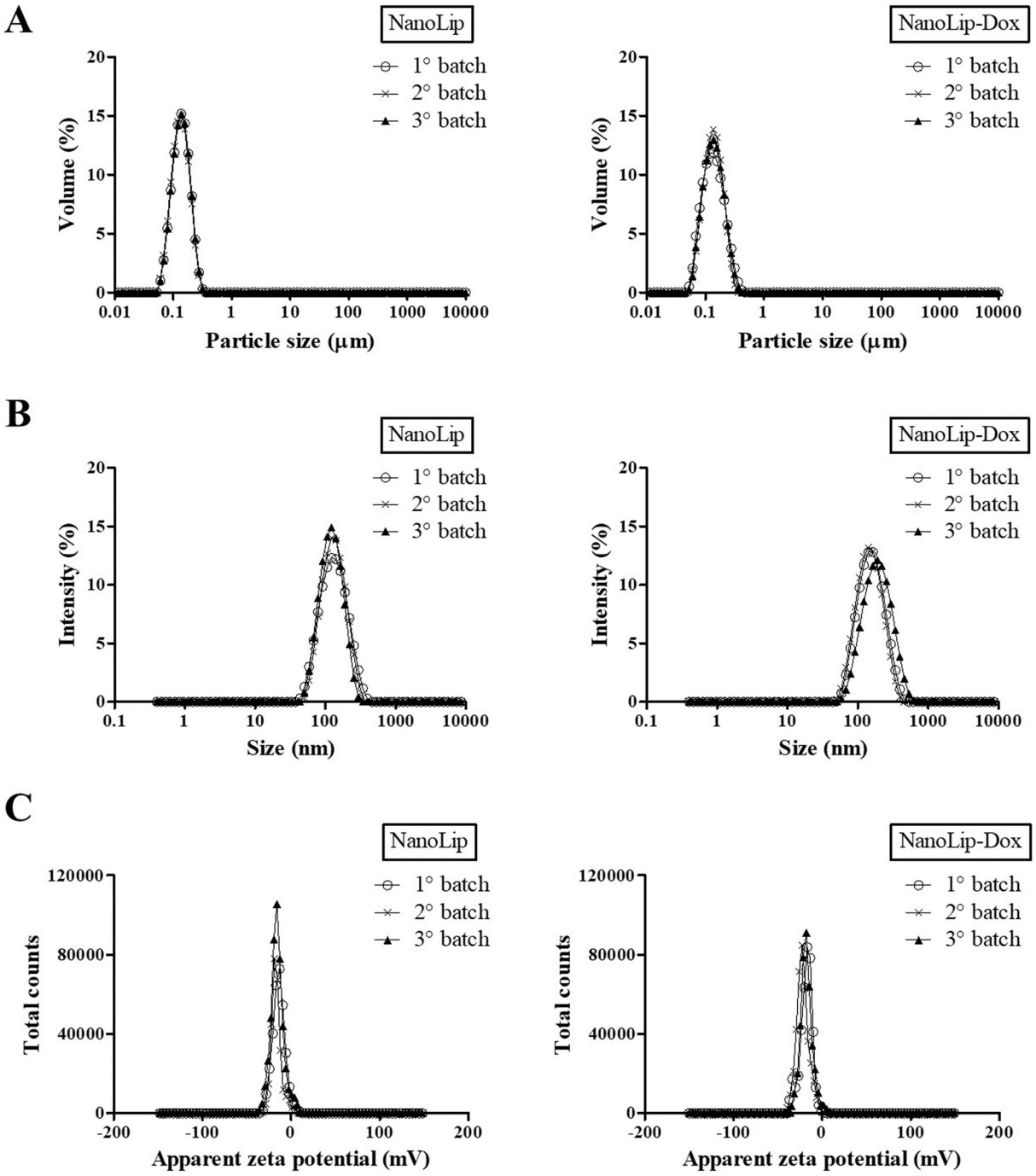

Fig. 2. Physicochemical characterization by nanoparticle tracking analysis of NanoLip and NanoLip-Dox *via* (A) laser diffraction, (B) dynamic light scattering, and (C) zeta potential determined by laser Doppler velocimetry.

(heart and liver) were harvested.

The organs were immediately fixed, dehydrated, cleared, embedded in paraffin, and stained with hematoxylin and eosin. The stained slides were observed under an optical microscope (Eclipse Si Microscope, Nikon, United States) to evaluate tissue responses to inflammation or damage ($n = 4$).

Biochemical analysis of hepatic enzymes was conducted using the collected amniotic fluids ($n = 4$). The amniotic liquids were centrifuged at 3000 $\times g$ for 10 min. The enzymatic activity of alanine aminotransferase (ALT) and aspartate aminotransferase (AST) were determined in the supernatants using the kinetic spectrophotometric method (AST/GOT Liquiform® and ALT/GPT® Liquiform, Labtest, Brazil).

2.4.2. Chicken embryo model for evaluating antitumor activity

A summary of the experimental design for antitumor evaluation using the chicken embryo model is shown in Fig. 1. The selection of the incubation protocol and establishment of the chicken embryo for cancer studies are described in the Supplementary Information. This model was previously developed ($n = 6$) under the following conditions: *ex ovo* cultures in a support film inside a plastic cup covered with a plastic Petri dish (see Fig. S1) and implantation of 5×10^6 cells/embryo (see Fig. S2 and Fig. S3). Human breast adenocarcinoma (MCF-7) cells were implanted on the surface of 7-day chicken CAM and the embryos were incubated in a climatic chamber (Nova Ética 420-CLD, Brazil) at 60% relative humidity and 37.5 °C until embryo development day 16. The

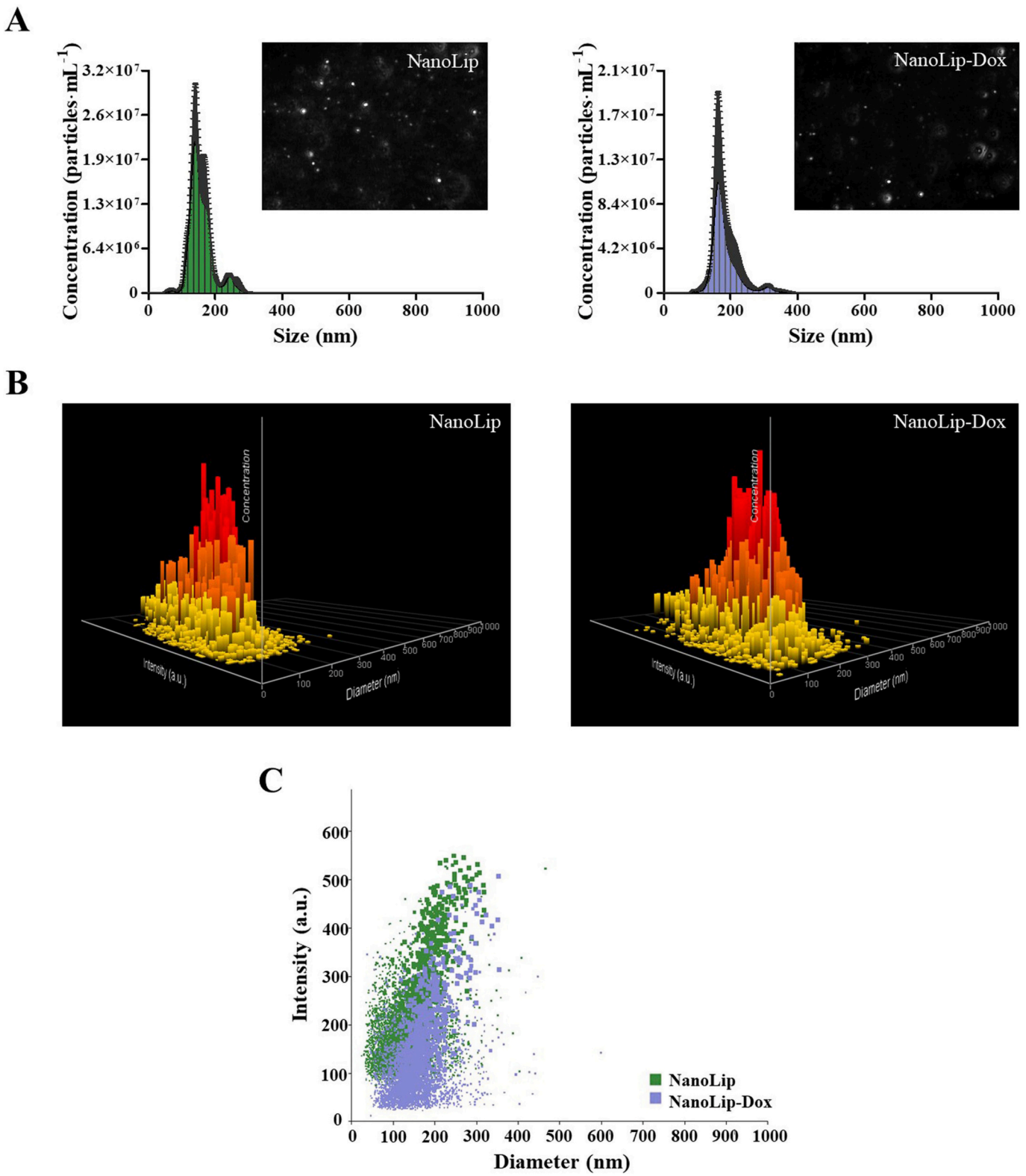

Fig. 3. Physicochemical characterization by nanoparticle tracking analysis of NanoLip and NanoLip-Dox. (A) Plots of particle size distribution by particle concentration expressed in mean ± standard deviation and sample video frame (right panels). (B) Three-dimensional plots (diameter *vs.* intensity *vs.* concentration). (C) Superposition of size profiles by intensity of scattered light for NanoLip and NanoLip-Dox formulations.

treatments (two doses) were administered directly over the developed tumor on embryo development days 10 and 13. Dox.HCl in solution or nanoencapsulated (NanoLip-Dox) was administered (30 μL) at a final concentration of 1.7 μmol·L^{-1} of drug salt. Treatment in the control group with tumor consisted of saline solution (30 μL).

Embryos were monitored daily until embryo development day 16 to verify the mortality ($n = 6$). The embryo survival rate was calculated as the percentage of survived embryos and the survival curves were

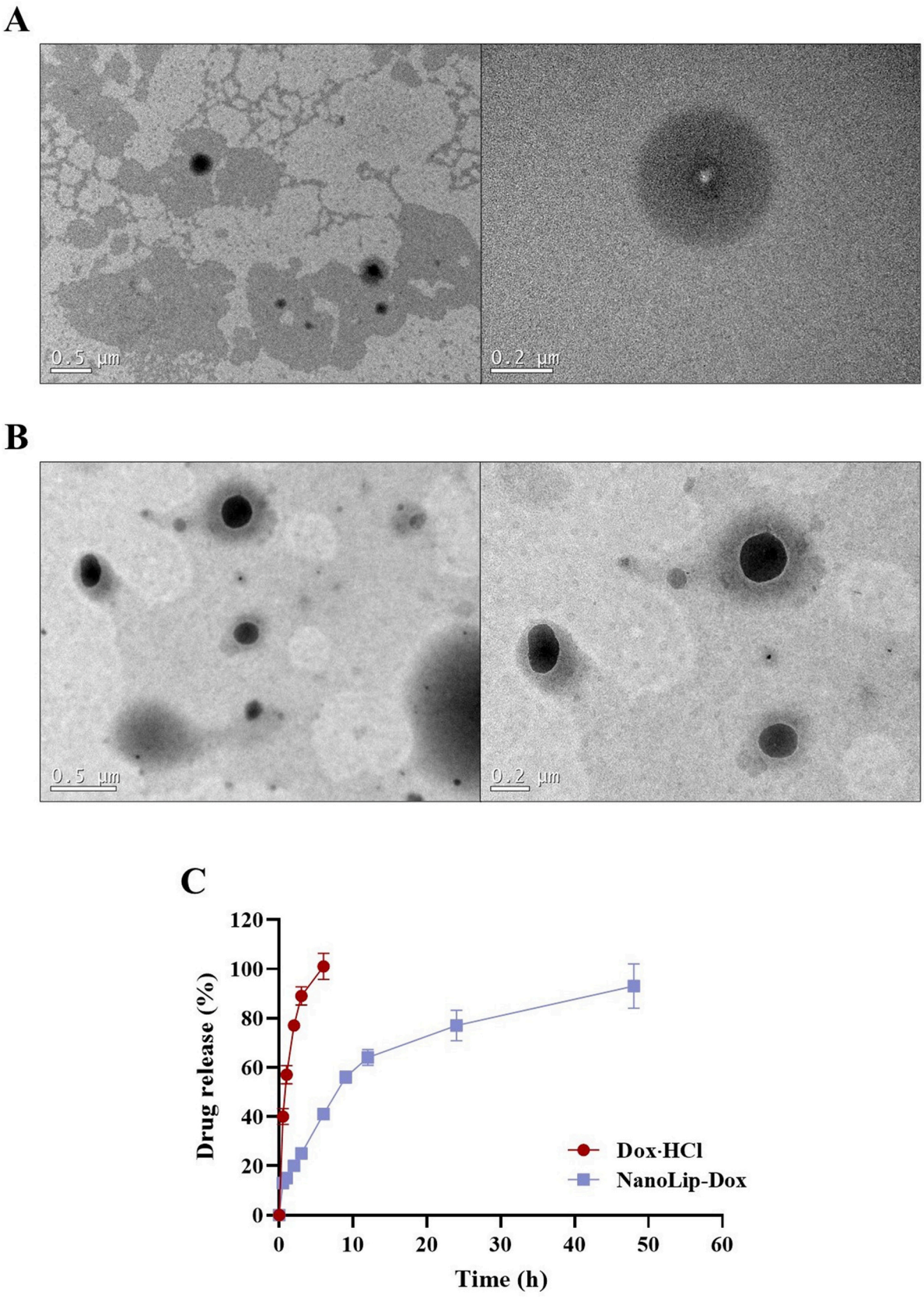

Fig. 4. Images obtained by transmission electron microscopy of (A) NanoLip and (B) NanoLip-Dox in bar scale of 0.5 µm (left) and 0.2 µm (right). (C) *In vitro* cumulative drug release by direct dialysis of Dox.HCl and NanoLip-Dox.

Table 2
Histological analysis for evaluating inflammation on a scale of 0–3 depending on the intensities of inflammatory infiltrate, hyperemia, and hemorrhage.

Sample	Inflammatory infiltrate	Hyperemia	Hemorrhage
Control	0.0 ± 0.0	0.0 ± 0.0	0.0 ± 0.0
NaOH 0.1 mol·L^{-1}	2.0 ± 0.5 *	2.0 ± 1.0	2.0 ± 1.0
Dox.HCl 862.1 μmol·L^{-1}	1.0 ± 0.5	0.0 ± 1.5	0.0 ± 1.0
Dox.HCl 172.4 μmol·L^{-1}	0.0 ± 0.5	0.0 ± 1.0	0.0 ± 0.0
Dox.HCl 34.5 μmol·L^{-1}	0.0 ± 0.0	0.0 ± 0.0	0.0 ± 0.0
NanoLip-Dox 172.4 μmol·L^{-1}	1.0 ± 0.5	0.0 ± 0.0	0.0 ± 0.0
NanoLip-Dox 86.2 μmol·L^{-1}	0.0 ± 0.0	0.0 ± 1.0	0.0 ± 0.0
NanoLip-Dox 34.5 μmol·L^{-1}	0.0 ± 0.0	0.0 ± 0.5	0.0 ± 0.0

Dox.HCl, doxorubicin hydrochloride; NanoLip-Dox, lipid nanocarrier containing doxorubicin.
Results are expressed as mean ± standard deviation ($n = 3$).
* Statistical difference in median ± interquartile range compared with the control group analyzed per column (Kruskal–Wallis test with Dunn's multiple comparison test, $p < 0.05$).

constructed. At the end of each experiment, the embryos were euthanized; and the blood, amniotic fluid, and tissues were harvested. Tumor size determination (see Table S1) and hematological (see Fig. S4), enzymatic activity (ALT, AST and creatinine) (see Table S2), morphological (see Fig. S5, Table S3 and Table S4), and histological analyses (Fig. S6) were performed as described in sections 1, 2, 3, and 4 of the Supplementary Information. Tumor remission was calculated from tumor sizes determined before ($TS_{initial}$) and after (TS_{final}) treatment according to Eq. (2).

$$Tumor\ remission\ (\%) = \frac{TS_{initial} - TS_{final}}{TS_{initial}} \times 100 \quad (2)$$

We also determined the micro-hematocrit *via* centrifugation (9000 ×*g* for 5 min) of capillary tubes filled with the embryos' blood.

2.5. Statistical analysis

Data were expressed as mean ± standard deviation. In the physicochemical characterization of nanoformulations, Student's *t*-test was used to define the significance between two groups. Regarding the *in vivo* evaluations, statistical analysis was performed using the ANOVA with Dunnett's multiple comparison test or Kruskal–Wallis test with Dunn's multiple comparison test. Differences were considered significant at $p < 0.05$.

3. Results

3.1. Development of new lipid nanocarrier containing doxorubicin

The NanoLip and NanoLip-Dox formulations were prepared by spontaneous emulsification. Their physicochemical characteristics including particle size, hydrodynamic diameter, zeta potential, particle concentration, drug content, and entrapment efficiency are listed in Table 1. Laser diffraction analysis revealed unimodal particle size distributions with D[4,3]v below 140 nm for both formulations (Fig. 2A). The z-average hydrodynamic diameter of NanoLip-Dox (144 ± 16 nm, $n = 3$) determined by dynamic light scattering was higher ($p < 0.05$) than that of NanoLip (117 ± 5 nm, $n = 3$) (Fig. 2B). In addition, the values of the span and PDI were approximately 1 and 0.2, respectively, indicating a narrow size distribution. The values of the zeta potential were slightly negative (−15.5 ± 1.3 and − 19.5 ± 2.5 mV, $n = 3$) (Fig. 2C), owing to the presence of oleic acid and polysorbate 80. The drug content was 0.099 mg·mL^{-1} (98.6 ± 2.2% theoretical value, $n = 3$) and the entrapment efficiency was 95.3 ± 2.6% ($n = 3$).

The mean hydrodynamic diameter of NanoLip-Dox (190.0 ± 2.0 nm, $n = 3$) determined by nanoparticle tracking analysis was also higher ($p < 0.05$) than that of the drug-unloaded formulation, NanoLip (160.1 ± 2.9 nm, $n = 3$) (Fig. 3A). The particle concentration was (6.2 ± 1.4) × 10^{12} particles·mL^{-1} ($n = 3$) for NanoLip and (3.0 ± 2.5) × 10^{12} particles·mL^{-1} ($n = 3$) for NanoLip-Dox (Fig. 3A and B). The particle distributions of the two formulations overlapped with the diameter per unit intensity (Fig. 3C). This overlap demonstrated the absence of drug crystals in the NanoLip-Dox sample, proving that drug saturation was not exceeded in this formulation (Jornada et al., 2012). Photomicrographs obtained by transmission electron microscopy for NanoLip (Fig. 4A) and NanoLip-Dox (Fig. 4B) showed nano-sized oil droplets. The drug release profile was analyzed by direct dialysis experiment (Fig. 4C). NanoLip-Dox presented 92.9 ± 9.1% of the drug released at 48 h, whereas Dox.HCl was totally dialyzed in 6 h. Mathematical modeling revealed that the best-fitted model to describe the dialysis profile of the drug was the bi-exponential model for Dox.HCl (MSC = 4.31 and $r = 0.9982$) and NanoLip-Dox (MSC = 3.70 and $r = 0.9968$). In addition, using the Korsmeyer-Peppas equation resulted in a value of 0.62 for the drug released from NanoLip-Dox. This value indicates that the drug release mechanism occurs by anomalous transport consisting of diffusion and erosion.

3.2. Chicken embryo model for toxicological evaluations

3.2.1. Evaluation of inflammatory response and cell damage in CAM

In the positive control group, inflammatory infiltrates were observed after NaOH administration (Table 2 and Fig. 5B). Hyperemia and hemorrhage were observed at comparatively lower intensities in this group. The administration of Dox.HCl in solution and NanoLip-Dox caused mild inflammation at high concentrations (862.1 and 172.4 μmol·L^{-1}, respectively) in an isolate case; however, in most CAM samples, inflammatory reactions were not observed (Fig. 5C and D).

Cell damage in the CAM was determined by the amount of trypan blue dye absorbed by the injured cells (negative control: 3.3 ± 0.7 nmol·L^{-1}). Similarly to the histological analysis, two groups with cellular damage were observed: NaOH solution (9.7 ± 2.7 nmol·L^{-1}) and free drug (10.4 ± 1.3 nmol·L^{-1}) at the highest concentration (862.1 μmol·L^{-1}) (Fig. 5E). Therefore, these both treatments were considered moderate irritants; whereas the other treatments were classified as non-irritant/weak irritants (values lower than 7.0 nmol·mL^{-1}), including NanoLip-Dox in all concentrations and Dox.HCl at low concentrations. NanoLip (blank formulation) was also considered non-irritant since a low amount of trypan blue (4.1 ± 1.7 nmol·L^{-1}) was absorbed after 100 μL of formulation administration on the CAM.

3.2.2. Determination of survival rate, hepatoxicity, and cardiotoxicity

Under the experimental conditions and concentrations used in the present study, none of the treatments caused 100% embryo death (Fig. 6A and B). After 96 h of treatment, the survival rate was 50% in the group that received Dox.HCl 1.7 μmol·L^{-1}. In contrast, the nanoformulation at the same concentration did not cause embryo death until the end of the experiment (Fig. 6B).

Hearts and livers of the embryos were collected and processed for histopathological evaluation (Fig. 6C). In the control group, we observed normal tissue architecture in all organs. Similarly, no morphological changes or inflammatory findings were observed in the other groups.

Hepatic enzymes in the amniotic fluid were analyzed (Table 3), because other studies have demonstrated the presence of these enzymes in this sample type (Khosravi et al., 2018a). Administration of the nanoformulation at five different concentrations did not increase the activity of hepatic enzymes compared to those in the control group. In contrast, Dox.HCl at higher concentrations (862.1, 344.8, and 172.4 μmol·L^{-1}) increased the level of AST (20.8 ± 3.2, 17.6 ± 3.5, and 17.4 ± 4.2 U/L, respectively).

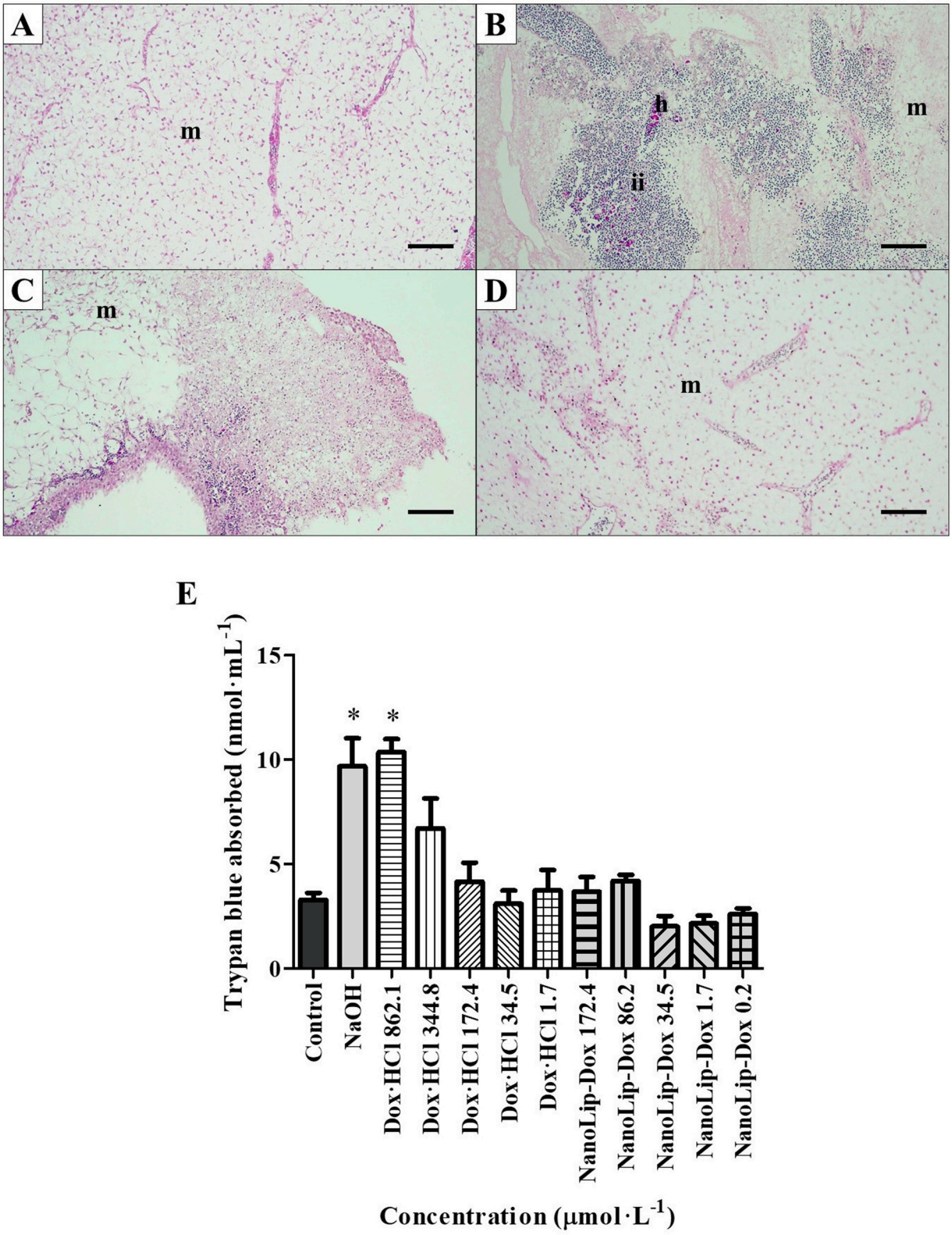

Fig. 5. Chorioallantoic membrane (CAM) analysis after administration of samples. Representative histological images of hematoxylin and eosin-stained CAMs from the (A) control group, (B) NaOH group, (C) Dox.HCl 862.1 μmol·L^{-1}, and (D) NanoLip-Dox 172.4 μmol·L^{-1} at 100× magnification (scale bar = 100 μm). (m) Mesoderm, (h) hemorrhage, and (ii) inflammatory infiltrate. (E) Cell damage in CAM evaluated by amount of trypan blue absorbed (nmol·mL^{-1}) by free drug (Dox.HCl) and NanoLip-Dox at five different drug concentrations ($n = 4$). Cell damage is observed after administration of NaOH (0.1 μmol·L^{-1}) and Dox.HCl 862.1 μmol·L^{-1} to CAM compared with that in the control group (ANOVA with Dunnett's multiple comparison test, $p < 0.05$). (For interpretation of the references to colour in this figure legend, the reader is referred to the web version of this article.)

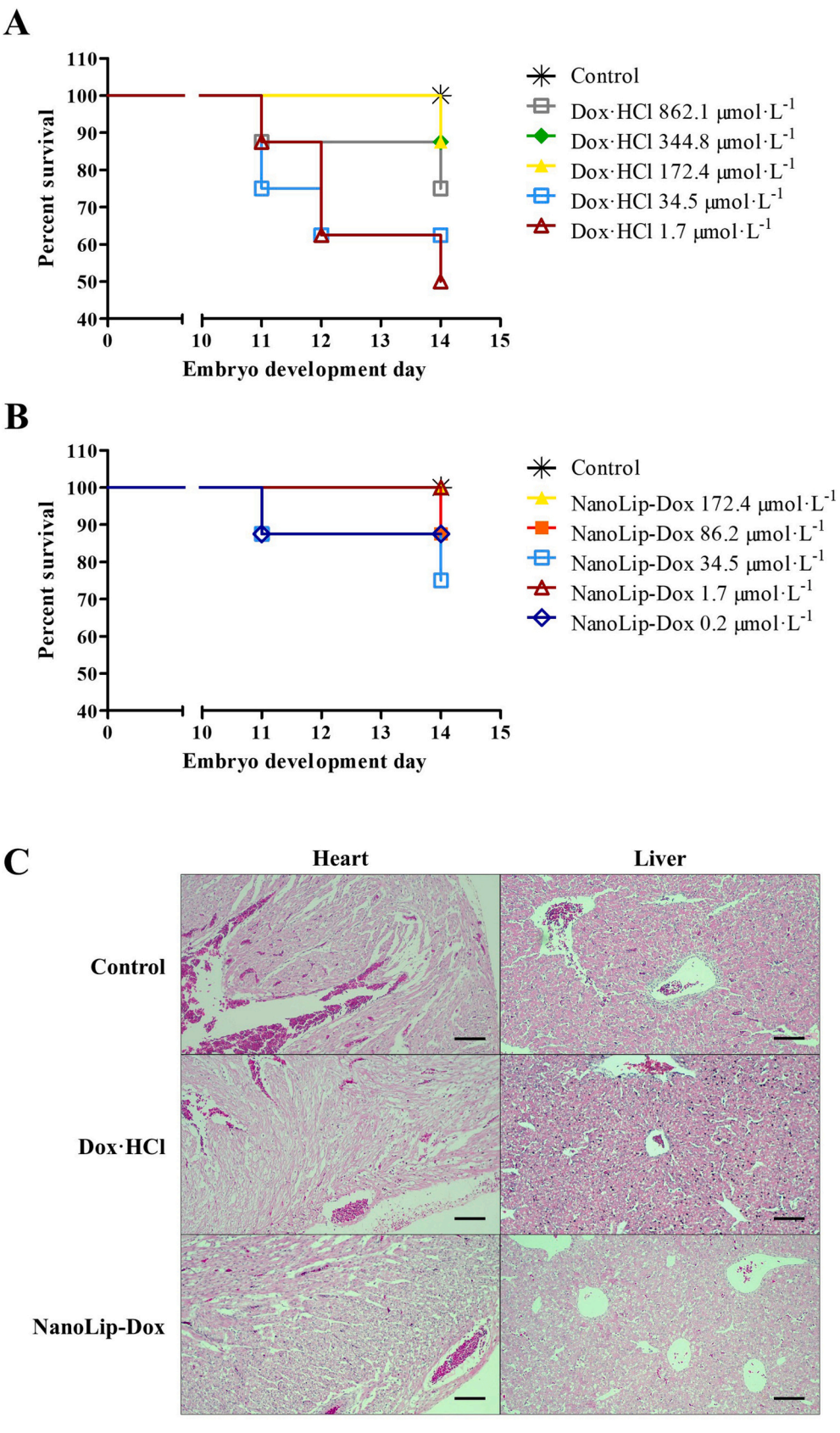

Fig. 6. Embryo survival rates after one dose of (A) Dox.HCl and (B) NanoLip-Dox at five different concentrations. Treatments were administered to the CAM on embryo development day 10 followed by monitoring until embryo development day 14 ($n = 8$ embryo per group). (C) Representative histological images of hematoxylin and eosin-stained heart and liver of the control group, Dox.HCl 862.1 μmol·L^{-1}, and NanoLip-Dox 172.4 μmol·L^{-1} at 100× magnification (scale bar = 100 μm). Normal structure of the heart and liver are seen.

Table 3
Analysis of the hepatic enzymes ALT and AST in amniotic fluid after administering Dox.HCl and NanoLip-Dox at different concentrations ($n = 4$).

Group	ALT (U/L)	AST (U/L)
Control	8.9 ± 3.2	10.0 ± 3.9
Dox.HCl 862.1 μmol·L^{-1}	13.5 ± 3.6	20.8 ± 3.2 *
Dox.HCl 344.8 μmol·L^{-1}	12.5 ± 2.0	17.6 ± 3.5 *
Dox.HCl 172.4 μmol·L^{-1}	8.3 ± 0.9	17.4 ± 4.2 *
Dox.HCl 34.5 μmol·L^{-1}	5.6 ± 2.5	14.7 ± 5.4
Dox.HCl 1.7 μmol·L^{-1}	6.9 ± 1.9	14.9 ± 2.9
NanoLip-Dox 172.4 μmol·L^{-1}	10.8 ± 4.6	10.9 ± 2.8
NanoLip-Dox 86.2 μmol·L^{-1}	7.5 ± 2.4	12.9 ± 2.3
NanoLip-Dox 34.5 μmol·L^{-1}	7.5 ± 3.5	10.7 ± 2.9
NanoLip-Dox 1.7 μmol·L^{-1}	10.8 ± 3.7	10.7 ± 2.1
NanoLip-Dox 0.2 μmol·L^{-1}	7.9 ± 2.9	12.1 ± 5.0

Dox.HCl, doxorubicin hydrochloride; NanoLip-Dox, lipid nanocarrier containing doxorubicin.

* Statistical difference in mean ± standard deviation in relation to the negative control group analyzed per column (ANOVA with Dunnett's multiple comparison test, $p < 0.05$).

3.3. Chicken embryo model for evaluation of antitumoral efficacy

We successfully optimized the protocols for stablishing the chicken embryo cancer model. Considering the use of *in ovo* or *ex ovo* cultures (see section 1 in the Supplementary Information, Fig. S1), optimization tumor cell concentration for implantation in the CAM (see sections 2 and 3 in the Supplementary Information, Fig. S2, Table S1, and Fig. S3), and analyzing several parameters related to embryo development (see section 4 in the Supplementary Information, Fig. S4, Table S2, Fig. S5, Table S3, Table S4, and Fig. S6).

After tumor development, the administration of two doses of NanoLip-Dox caused a high tumor remission percentage (40.9 ± 9.7%), differing ($p < 0.05$) from that of the control group with tumor (8.6 ± 14.8%) (Fig. 7A and C). In contrast, Dox.HCl resulted in a tumor remission percentage (20.7 ± 21.0%) similar to that of the control group ($p > 0.05$). Another interesting finding was the survival rate of the embryos after treatment. We observed that nanoencapsulated doxorubicin was less toxic to embryos because no embryo died until the end of the experiment (survival rate of 100%). In contrast, Dox.HCl caused a survival rate of 66.7% until the end of the experiment (Fig. 7B). Histological analysis demonstrated that the tumor cells were densely packed inside Geltrex™ in the mesoderm (Fig. 7C).

Blood smear analysis demonstrated normality in blood cells with no signs of inflammation in all groups (Fig. 8A), and the hematocrit was similar in all groups ($p > 0.05$) (Table 4). The morphological measurements and weights of embryos and organs did not show a statistical difference between the treatment and control groups (Table 4). Concerning enzymes, the statistical analyses demonstrated equality between groups; however, the enzymatic activity of ALT (40.1 ± 58.3 U/L, $p = 0.24$) and AST (114.3 ± 230.9 U/L, $p = 0.48$) tended to increase after Dox.HCl treatment (Table 4). Histopathological analysis of the heart revealed normal tissue architecture in all groups (Fig. 8B). In contrast, discrete hyperemia was observed in the liver after Dox.HCl treatment, but not after NanoLip-Dox treatment (Fig. 8C). Collectively, these results indicated the higher safety and efficacy of NanoLip-Dox than those of the drug in solution.

4. Discussion

Nanodelivery of chemotherapeutics is an important strategy to decrease their commonly reported side and toxic effects. Nanocarried-doxorubicin is available for clinical use in pegylated (Doxil® or Caelyx®) and non-pegylated (Myocet®) liposomal membrane of phosphatidylcholine and cholesterol (Leonard et al., 2009). The drug loading occurs by the transmembrane gradient of ammonium sulfate in the Doxil®; in the Myocet® the doxorubicin is loaded into liposomes in the moment of its clinical use (Liu et al., 2022). The drug loading for Doxil® is very low (11%), and a poor drug release is reported (Barenholz, 2012). The non-pegylated liposomes are phagocytized by mononuclear phagocytes; on the other hand, target cells can interact less with pegylated liposomes and, consequently, decrease cell internalization (Leonard et al., 2009; Liu et al., 2022). In this study, we developed a new lipid nanocarrier for doxorubicin with globules composed of caprylic/capric triglyceride and sorbitan monostearate, resulting in high drug loading and a controlled release profile.

Sorbitan monostearate is a nonionic surfactant with a low molecular mass and low hydrophilic–lipophilic balance. It can act as an organic gelator for various vegetable oils, including caprylic/capric triglyceride (Murdan et al., 1999). This organogel has a three-dimensional network structure of tubules with thermoreversible properties (Sahoo et al., 2011). In lipid-core nanocapsules, sorbitan monostearate is well known to be dispersed in caprylic/capric triglyceride, acting as an organic gelator (Poletto et al., 2015). It modifies the characteristics of the nanocapsule pseudophases, mainly by increasing the drug-loading capacity of the nanoformulations (Poletto et al., 2015). This organogel is affected by the presence of a hydrophilic surfactant, which improves gel stability (Murdan et al., 1999). Polysorbate 80 is a hydrophilic surfactant that together with lecithin, physically stabilizes globules dispersed in water. Thus, both surfactants can form hydrophilic coronas in nanoformulations (Cé et al., 2016). Oleic acid was chosen in this study because it can form an organic salt with doxorubicin, which does not dissociate in water and has antitumor effects (Delgado et al., 2015; Jiang et al., 2017). In addition, doxorubicin can form a complex with oleic acid, which is more lipophilic than the free drug, facilitating its nanoencapsulation (Munnier et al., 2007).

The chicken embryo model has been demonstrated to be appropriate for many scientific purposes such as *in vivo* toxicological evaluations for the selection of new nanocarriers (Kensova et al., 2015; Buteică et al., 2016; Kurantowicz et al., 2017; Nazaktabar et al., 2017; Patel et al., 2019; Carvalho et al., 2021). In the present study, we did not observe any toxic effects in normal tissues following NanoLip-Dox administration to chicken embryos in terms of several parameters and concentrations. In contrast, Dox.HCl in solution showed some toxicological effects after administration to CAM. Toxicological and safety studies are important to evaluate both free and nanoencapsulated drugs. They provide information on interactions between living systems and their possible deleterious effects. CAM is an extra-embryonic membrane related to embryo circulation, comprising complete tissue with rich vascularization (capillaries, arteries, and veins) and inflammatory responses (McKenzie et al., 2015; Victorelli et al., 2020; Kundeková et al., 2021;). Thus, treatments administered to the CAM are absorbed and reach the systemic circulatory system, which can affect the normal development of chick embryos (Ribatti, 2017).

Therefore, the parameters related to CAM, including inflammation and cell damage, were evaluated. In both analyses, we used the NaOH solution as a positive control, which resulted in intense inflammation and cell damage. NaOH solution is commonly considered a standard for irritation and inflammation in the HET-CAM assay (McKenzie et al., 2015; Sousa et al., 2017; Palmeira-de-Oliveira et al., 2018). Dox.HCl at a high concentration (862.1 μmol·L^{-1}) caused moderate inflammation, based on histological analyses and cellular damage evaluated by trypan blue absorption. Doxorubicin is commonly reported to cause irritation and other cutaneous reactions (Fabbrocini et al., 2012).

Interestingly, the survival rates of embryos until embryo development day 14 were independent of the dose. The Dox.HCl in solution group at concentrations 862.1, 344.8, and 172.4 μmol·L^{-1} showed survival rates higher than 70%. Concurrently, the lowest concentrations (34.5 and 1.7 μmol·L^{-1}) resulted in survival rates of 62.5% and 50%, respectively. For the nanoformulation at the same concentrations as in solution (34.5 and 1.7 μmol·L^{-1}), the survival rates were 75% and 100%, respectively. This parameter clearly verified the influence of nanoencapsulation on decreasing embryotoxicity. We also observed that

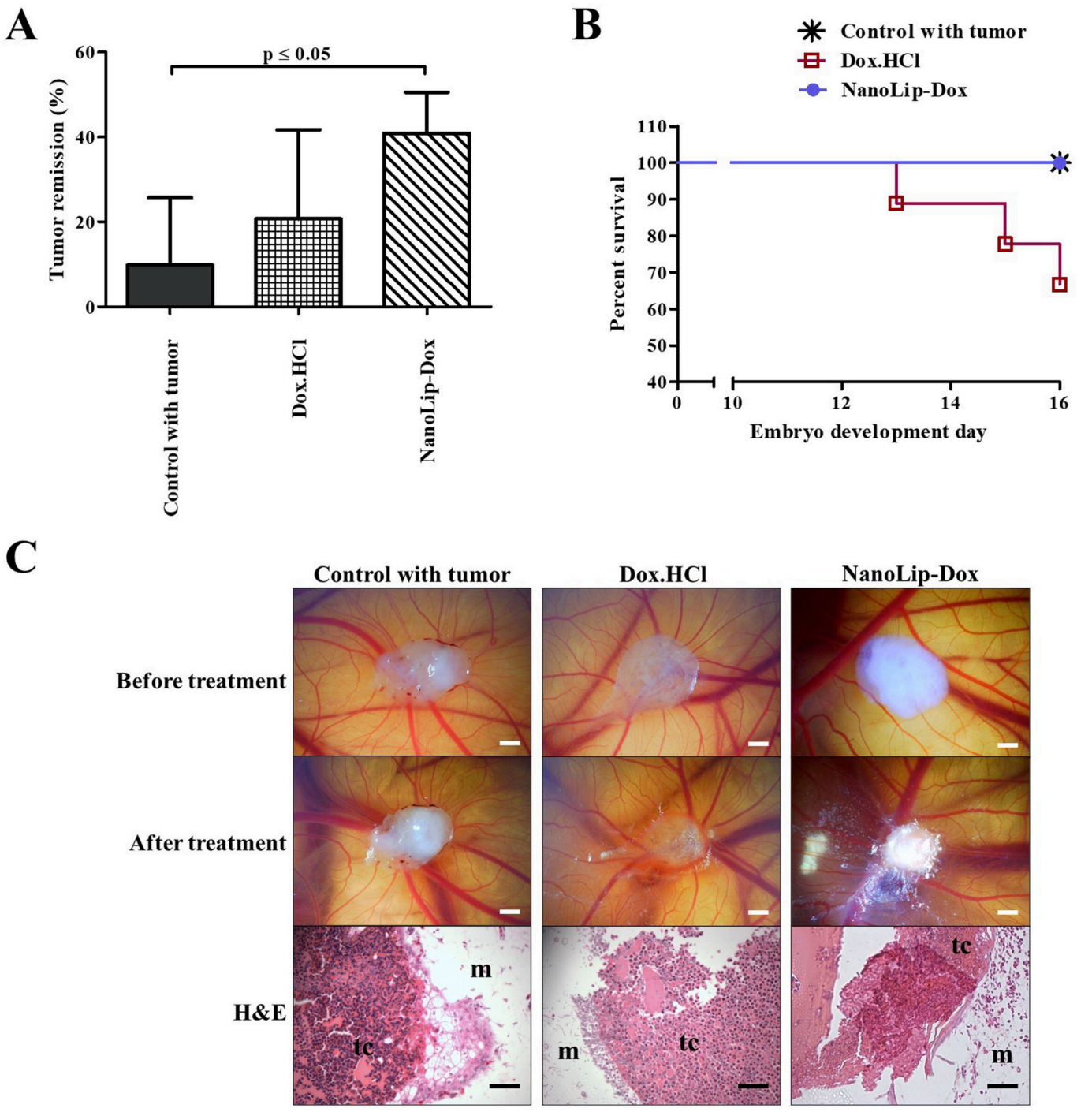

Fig. 7. (A) Antitumor activity after two doses at 1.7 μmol·L^{-1} Dox.HCl ($n = 9$*) in solution and nanoencapsulated (NanoLip-Dox, $n = 6$) administered in the tumor on chorioallantoic membrane (CAM). Results expressed in mean ± standard deviation (ANOVA with Dunnett's post-hoc test) compared to the control group with tumor (n = 6). *Three embryos from this group died and their tumor remission rates were considered 0%. (B) Percent survival of embryos in the control group with tumor (n = 6) and after two doses at 1.7 μmol·L^{-1} Dox.HCl (n = 9) in solution or nanoencapsulated (NanoLip-Dox, n = 6) administered in the tumor on CAM. (C) Representative images of CAM with tumor obtained before and after treatment (scale bars = 1 mm), and representative images of CAM with tumor after treatment stained with hematoxylin and eosin at 400× magnification (scale bars = 50 μm). (tc) Tumor cells densely packed inside Geltrex™ and (m) mesoderm.

at higher concentrations of Dox.HCl in solution, more embryos survived than at lower concentrations. This can be related to the aggregation state of doxorubicin, in which the drug is more soluble at low concentrations, permeating better through the CAM and reaching the embryo. Another theory explaining this result is that the embryo adopts different defense mechanisms. The determined survival rate data could be useful in correlating with other *in vivo* models. In another study, the median lethal doses obtained from this model and databases of mice for one-dose administrations of diverse chemotherapy drugs to the CAM allantoic artery of chicken embryos were significantly correlated (Kue et al., 2015).

AST and ALT enzymes were also quantified in the amniotic fluid, which is easy to collect and can be obtained in larger volumes than blood. The amniotic fluid is an indicator of the health of an embryo during development (Khosravi et al., 2018b). Histological analyses of the organs (hearts and livers) did not reveal any toxicological findings in

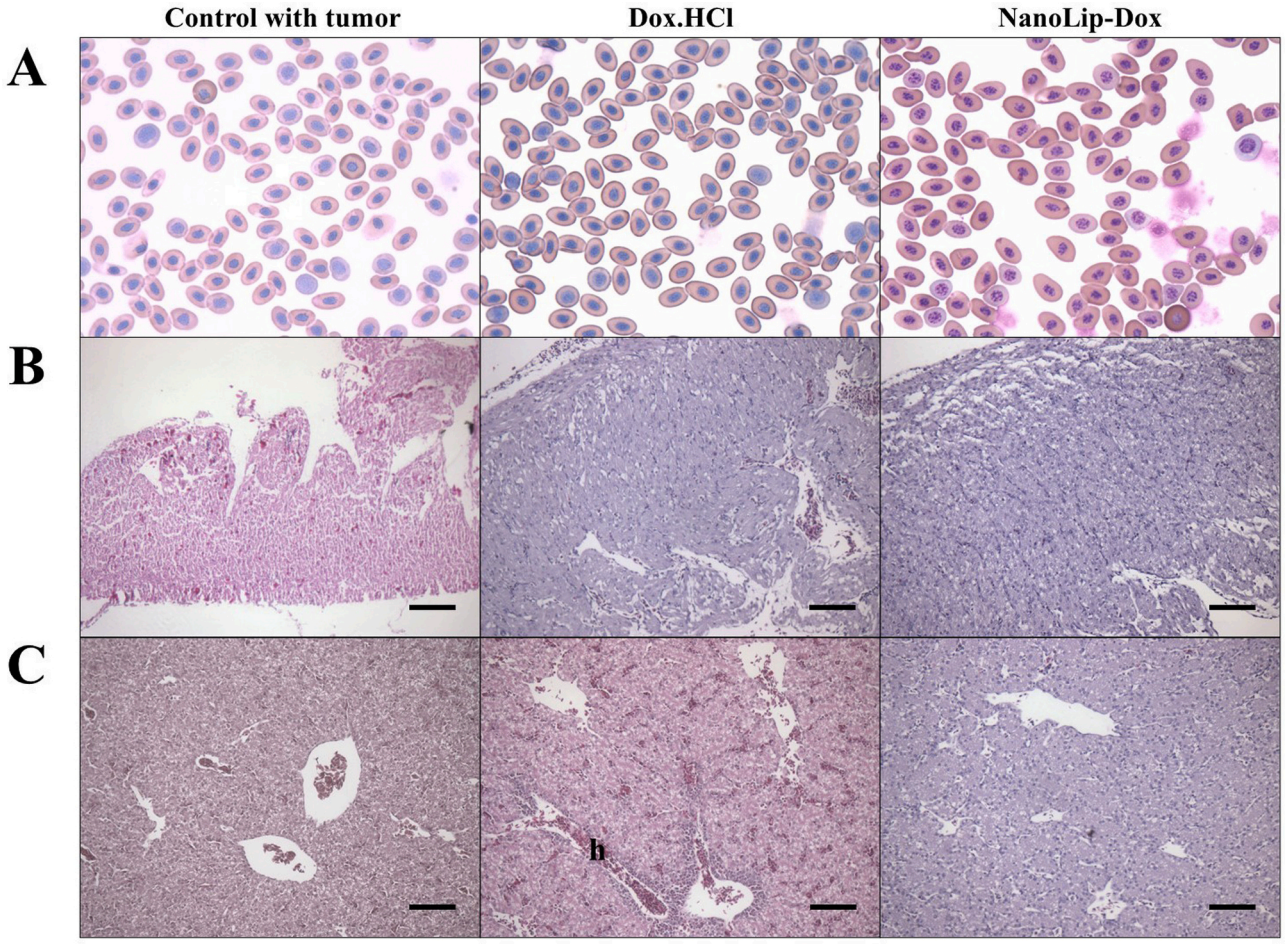

Fig. 8. (A) Representative images of blood smear stained by fast panoptic technique with modifications at 1000× magnification. Representative images of histological sections stained with hematoxylin & eosin from (B) heart and (C) liver at 200× magnification (scale bars = 100 μm). Normal structures of the heart and liver are seen after treatment with NanoLip-Dox. Normal structure of the heart and (h) discrete hyperemia are seen after treatment with Dox.HCl.

Table 4
Hematocrit, enzymatic activity (ALT, AST, and creatinine), morphological analyses, and embryos and organs weights after MCF-7 cells implantation and treatment administration ($n = 6$).

Parameter	Control with tumor	Dox.HCl	NanoLip-Dox
Hematocrit (%)	28.9 ± 2.3	28.0 ± 2.0	32.3 ± 5.0
ALT (U/L)	10.7 ± 3.0	40.1 ± 58.3	14.4 ± 3.1
AST (U/L)	23.2 ± 14.2	114.3 ± 230.9	21.2 ± 11.1
Creatinine (mg/dL)	0.3 ± 0.1	0.6 ± 0.4	0.3 ± 0.3
Total length (cm)	8.7 ± 0.4	8.8 ± 0.6	9.1 ± 0.5
Wing (cm)	1.7 ± 0.1	1.9 ± 0.2	1.8 ± 0.1
Beak (cm)	0.6 ± 0.1	0.7 ± 0.1	0.7 ± 0.1
Leg (cm)	1.9 ± 0.3	2.2 ± 0.3	2.0 ± 0.1
Middle finger (cm)	1.0 ± 1.1	1.1 ± 0.2	1.0 ± 1.1
Embryo weigh (g)	9.5 ± 1.4	10.5 ± 2.9	9.9 ± 1.3
Heart weigh (g)	0.10 ± 0.01	0.11 ± 0.03	0.10 ± 0.03
Liver weigh (g)	0.21 ± 0.05	0.21 ± 0.07	0.17 ± 0.08
Kidneys weigh (g)	0.03 ± 0.01	0.03 ± 0.02	0.02 ± 0.01

Dox.HCl, doxorubicin hydrochloride; NanoLip-Dox, lipid nanocarrier containing doxorubicin; ALT, alanine aminotransferase; AST, aspartate aminotransferase. Mean ± standard deviation analyzed per line. All groups showed statistical equality for each parameter compared with the control group (ANOVA with Dunnett's post-hoc test, $p < 0.05$).

any of the groups. However, the biochemistry of hepatic enzymes demonstrated an increase in the AST level after administrating Dox.HCl at 862.1, 344.8, and 172.4 μmol·L^{-1}. This increase suggests hepatocellular disruption associated with recent liver injury (Khosravi et al., 2018b). This result corroborates with other studies that have reported that this drug can cause hepatotoxicity (Tulubas et al., 2015; Sesarman et al., 2021). Shingadia (2015) administered the commercial form of doxorubicin (Adriamycin®) (70 μg/egg) by injection into the air sac with increased level of AST. NanoLip-Dox at the same concentration (172.4 μmol·L^{-1}) maintained normal activity of hepatic enzymes.

Furthermore, the chicken embryo model has been used as a tumor model (Schomann et al., 2013; Cloney and Franz-Odendaal, 2015; Augustine et al., 2020) with few studies using the MCF-7 cell line (Liu et al., 2015; Chen et al., 2018; Kim et al., 2019). Here, we established of this model using the MCF-7 cell line while considering several parameters related to tumor and embryo development, demonstrating satisfactory and reproducible results. In this cancer model, we used *ex ovo* cultures owing to lower risk of microbial contamination, better visualization of tumor cell implantation, and control of tumor growth over time. Furthermore, we also evaluated the characteristics of embryo development, which are not commonly reported in the literature. However, considering that antitumor drugs can cause toxicity and/or adverse effects, an *in vivo* cancer model should also consider the embryo. Evaluating the efficacy of the NanoLip-Dox formulation in this tumor model, we observed potent antitumor activity with a high tumor remission percentage (40.9 ± 9.7%, $p < 0.05$) compared to the control group. In addition, the improvement in the survival rate compared to that of the drug salt in solution, the absence of toxicity concerning morphological characteristics, weights of embryos and organs, hematologic parameters, and enzymatic activity (ALT, AST, and creatinine) suggest the safety and efficacy of NanoLip-Dox.

5. Conclusions

The developed nanocarrier demonstrated a reduction in the toxicity of doxorubicin in normal tissues, mainly lower hepatotoxicity and improved survival rate of embryos. An increase in the survival rate of embryos was also observed when tumors were implanted to CAM of embryos. Furthermore, the nanoformulation showed a potent antitumor efficacy. The chicken embryo model also proved to be an interesting alternative for substituting or reducing animal experimentation in acute toxicity studies and for evaluating the antitumoral activity of drugs in solution and nanoencapsulated drugs. In light of these findings of safeness and efficacy, NanoLip-Dox can be a promising nanomedicine for the treatment of breast cancer.

Funding

This study was financed in part by the National Council for Scientific and Technological Development (CNPq, grant numbers 156042/2018-5, 164934/2020-0, and 305301/2014-4), the Research Support Foundation of Rio de Grande do Sul State (FAPERGS, grant number 17/2551-0001002-7 and PRONEX FAPERGS-CNPq grant number 16/2551-0000467-6), and the National Institute of Pharmaceutical Nanotechnology (INCT/Nanofarma, grant number 465687/2014-8).

Author contributions

ACS Alves was responsible for the conceptualization, methodology, formal analysis, data curation, writing- original draft preparation, visualization, and investigation. DR Dallemole and TM Ciocheta conducted the methodology, writing- original draft preparation, visualization, and investigation. Weber AF, Gündel SS, and F Visioli contributed to the methodology, visualization, and investigation. SS Guterres and Figueiró F contributed to the resources and funding acquisition. AR Pohlmann was responsible for the conceptualization, writing- original draft preparation, resources, funding acquisition, and supervision.

Declaration of Competing Interest

The authors declare the following financial interests/personal relationships which may be considered as potential competing interests:

Aline de Cristo Soares Alves reports financial support was provided by National Council for Scientific and Technological Development. Adriana Raffin Pohlmann reports financial support was provided by National Council for Scientific and Technological Development. Silvia Guterres reports financial support was provided by Foundation for Research Support of Rio Grande do Sul State. Adriana Raffin Pohlmann reports financial support was provided by State of Sao Paulo Research Foundation. Adriana Raffin Pohlmann potential conflit: IJP Associate Editor.

Data availability

Data will be made available on request.

Acknowledgements

The authors would like to thank Professor Sergio Luiz Vieira (Aviário de Ensino e Pesquisa do Departamento de Zootecnia, Universidade Federal do Rio Grande do Sul) for the eggs used in the study and CAPES and CNPq for their fellowships.

Appendix A. Supplementary data

Supplementary data to this article can be found online at https://doi.org/10.1016/j.ijpx.2023.100193.

References

Abed, A.R., Ibraheem, A.F., Abbas, H.A., 2020. Embryogenic effects of doxorubicin in chicken embryo. Curr. Top. Pharmacol. 24, 99–104.

Alavi, M., Nokhodchi, A., 2020. Microformulations and nanoformulations of doxorubicin for improvement of its therapeutic efficiency. Crit. Rev. Ther. Drug Carrier Syst. 37, 591–611. https://doi.org/10.1615/CritRevTherDrugCarrierSyst.2020034470.

Aleksandar, P., Dragana, M.-Ć., Nebojša, J., Biljana, N., Nataša, S., Branka, V., Jelena, K.-V., 2019. Wild edible onions - *Allium flavum* and *Allium carinatum* - successfully prevent adverse effects of chemotherapeutic drug doxorubicin. Biomed. Pharmacother. 109, 2482–2491. https://doi.org/10.1016/j.biopha.2018.11.106.

Al-Malky, H.S., Harthi, S.E.A., Osman, A.-M.M., 2020. Major obstacles to doxorubicin therapy: cardiotoxicity and drug resistance. J. Oncol. Pharm. Pract. 26, 434–444. https://doi.org/10.1177/1078155219877931.

Andersen, C.L., Liu, M., Wang, Z., Ye, X., Xiao, S., 2019. Chemotherapeutic agent doxorubicin alters uterine gene expression in response to estrogen in ovariectomized CD-1 adult mice. Biol. Reprod. 100, 869–871. https://doi.org/10.1093/biolre/ioy259.

Antonow, M.B., Asbahr, A.C.C., Raddatz, P., Beckenkamp, A., Buffon, A., Guterres, S.S., Pohlmann, A.R., 2017. Liquid formulation containing doxorubicin-loaded lipid-core nanocapsules: cytotoxicity in human breast cancer cell line and *in vitro* uptake mechanism. Mater. Sci. Eng. C Mater. Biol. Appl. 76, 374–382. https://doi.org/10.1016/j.msec.2017.03.099.

Augustine, R., Alhussain, H., Hasan, A., Ahmed, M.B., Yalcin, H.C., Al Moustafa, A.-E., 2020. A novel *in ovo* model to study cancer metastasis using chicken embryos and GFP expressing cancer cells. Bosn. J. Basic. Med. Sci. 20, 140–148. https://doi.org/10.17305/bjbms.2019.4372.

Barenholz, Y., 2012. Doxil(R) – the first FDA-approved nano-drug: lessons learned. J. Control. Release 160, 117–134. https://doi.org/10.1016/j.jconrel.2012.03.020.

Blasi, P., Schoubben, A., Traina, G., Manfroni, G., Barberini, L., Alberti, P.F., Cirotto, C., Ricci, M., 2013. Lipid nanoparticles for brain targeting III. Long-term stability and *in vivo* toxicity. Int. J. Pharm. 454, 316–323. https://doi.org/10.1016/j.ijpharm.2013.06.037.

Borišev, I., Mrđanovic, J., Petrovic, D., Seke, M., Jović, D., Srđenović, B., Latinovic, N., Djordjevic, A., 2018. Nanoformulations of doxorubicin: how far have we come and where do we go from here? Nanotechnology. 29, 332002 https://doi.org/10.1088/1361-6528/aac7dd.

Buteică, S.A., Mihăiescu, D.E., Rogoveanu, I., Mărgăritescu, D.N., Mîndrilă, I., 2016. Chick chorioallantoic membrane model as a preclinical tool for nanoparticles biology study. Rom. Biotechnol. Lett. 21, 11684–11690.

Carvalho, F.B., Gomes, M.G., Savall, A.S.P., Fidelis, E.M., Pinton, S., Ribeiro, A.C.F., Munieweg, R., Oelke, C.A., Haas, S.E., 2021. Evaluation of curcumin-loaded polymeric nanocapsules with different coatings in chick embryo model: influence on angiogenesis, teratogenesis and oxidative stress. Pharmacol. Rep. 73, 563–573. https://doi.org/10.1007/s43440-021-00218-2.

Cé, R., Marchi, J.G., Bergamo, V.Z., Fuentefria, A.M., Lavayen, V., Guterres, S.S., Pohlmann, A.R., 2016. Chitosan-coated dapsone-loaded lipid-core nanocapsules: growth inhibition of clinical isolates, multidrug-resistant *Staphylococcus aureus* and *Aspergillus* ssp. Colloids Surf. A Physicochem. Eng. Asp. 511, 153–161. https://doi.org/10.1016/j.colsurfa.2016.09.086.

Chapman, K.L., Holzgrefe, H., Black, L.E., Brown, M., Chellman, G., Copeman, C., Couch, J., Creton, S., Gehen, S., Hoberman, A., Kinter, L.B., Madden, S., Mattis, C., Stemple, H.A., Wilson, S., 2013. Pharmaceutical toxicology: designing studies to reduce animal use, while maximizing human translation. Regul. Toxicol. Pharmacol. 66, 88–103. https://doi.org/10.1016/j.yrtph.2013.03.001.

Chen, J., Zhou, Z., Yao, Y., Dai, J., Zhou, D., Wang, L., Zhang, Q.-Q., 2018. Dipalmitoylphosphatidic acid inhibits breast cancer growth by suppressing angiogenesis via inhibition of the CUX1/FGF1/HGF signalling pathway. J. Cell. Mol. Med. 22, 4760–4770. https://doi.org/10.1111/jcmm.13727.

Chen, L., Wang, S., Feng, Y., Zhang, J., Du, Y., Zhang, J., Du, Y., Zhang, J., Ongeval, C.V., Ni, Y., Li, Y., 2021. Utilisation of chick embryo chorioallantoic membrane as a model platform for imaging-navigated biomedical research. Cells. 10, 463. https://doi.org/10.3390/cells10020463.

Cloney, L., Franz-Odendaal, T.A., 2015. Optimized *ex-ovo* culturing of chick embryos to advanced stages of development. J. Vis. Exp. 95, 52129. https://doi.org/10.3791/52129.

Delgado, Y., Morales-Cruz, M., Figueroa, C.M., Hernández-Román, J., Hernández, G., Griebenow, K., 2015. The cytotoxicity of BAMLET complexes is due to oleic acid and independent of the α-lactalbumin component. FEBS Open Bio. 5, 397–404. https://doi.org/10.1016/j.fob.2015.04.010.

Fabbrocini, G., Cameli, N., Romano, M.C., Mariano, M., Panariello, L., Bianca, D., Monfrecola, G., 2012. Chemotherapy and skin reactions. J. Exp. Clin. Cancer Res. 31, 50. https://doi.org/10.1186/1756-9966-31-50.

Fonseca, B.B., Silva, M.V., Ribeiro, L.N.M., 2021. The chicken embryo as an *in vivo* experimental model for drug testing: advantages and limitations. Lab. Anim. (NY). 50, 138–139. https://doi.org/10.1038/s41684-021-00774-3.

Honda, N., Kariyama, Y., Hazama, H., Ishii, T., Kitajima, Y., Inoue, K., Ishizuka, M., Tanaka, T., Awazu, K., 2015. Optical properties of tumor tissues grown on the chorioallantoic membrane of chicken eggs: tumor model to assay of tumor response to photodynamic therapy. J. Biomed. Opt. 20, 125001 https://doi.org/10.1117/1.JBO.20.12.125001.

Huang, W., Arai, F., Kawahara, T., 2015. Egg-in-cube: design and fabrication of a novel artificial eggshell with functionalized surface. PLoS One 10, e0118624. https://doi.org/10.1371/journal.pone.0118624.

Jiang, L., Wang, W., He, Q., Wu, Y., Lu, Z., Sun, J., Liu, Z., Shao, Y., Wang, A., 2017. Oleic acid induces apoptosis and autophagy in the treatment of tongue squamous cell carcinomas. Sci. Rep. 7, 11277. https://doi.org/10.1038/s41598-017-11842-5.

Jornada, D.S., Fiel, L.A., Bueno, K., Gerent, J.F., Petzhold, C.L., Beck, R.C.R., Guterres, S. S., Pohlmann, A.R., 2012. Lipid-core nanocapsules: mechanism of self-assembly, control of size and loading capacity. Soft Matter 8, 6646–6655. https://doi.org/10.1039/C2SM25754H.

Kensova, R., Blazkova, I., Vaculovicova, M., Milosavljevic, V., Blazkova, L., Hynek, D., Kopel, P., Novotna, M., Zehnalek, J., Pohanka, M., Trnkova, L., Adam, V., Kizek, R., 2015. The effect of cadmium ions and cadmium nanoparticles on chicken embryos and evaluation of organ accumulation. Int. J. Electrochem. Sci. 10, 3623–3634.

Khosravi, A., Sharifi, I., Tavakkoli, H., Keyhani, A.R., Afgar, A., Salari, Z., Mosallanejad, S.S., Bamorovat, M., Sharifi, F., Hassanzadeh, S., Sadeghi, B., Dabiri, S., Mortazaeizdeh, A., Sheikhshoaie, Z., Salarkia, E., 2018a. Vascular apoptosis associated with meglumine antimoniate: *in vivo* investigation of a chick embryo model. Biochem. Biophys. Res. Commun. 505, 794–800. https://doi.org/10.1016/j.bbrc.2018.09.152.

Khosravi, A., Sharifi, I., Tavakkoli, H., Derakhshanfar, A., Keyhani, A.R., Salari, Z., Mosallanejad, S.S., Bamorovat, M., 2018b. Embryonic toxico-pathological effects of meglumine antimoniate using a chick embryo model. PLoS One 13, e0196424. https://doi.org/10.1371/journal.pone.0196424.

Kim, J.W., Gautam, J., Kim, J.E., Kim, J.-A., Kang, K.W., 2019. Inhibition of tumor growth and angiogenesis of tamoxifen-resistant breast cancer cells by ruxolitinib, a selective JAK2 inhibitor. Oncol. Lett. 17, 3981–3989. https://doi.org/10.3892/ol.2019.10059.

Kucinska, M., Murias, M., Nowak-Sliwinska, P., 2017. Beyond mouse cancer models: three-dimensional human-relevant *in vitro* and non-mammalian *in vivo* models for photodynamic therapy. Mutat. Res. 773, 242–262. https://doi.org/10.1016/j.mrrev.2016.09.002.

Kue, C.S., Tan, K.Y., Lam, M.L., Lee, H.B., 2015. Chick embryo chorioallantoic membrane (CAM): an alternative predictive model in acute toxicological studies for anti-cancer drugs. Exp. Anim. 64, 129–138. https://doi.org/10.1538/expanim.14-0059.

Kundeková, B., Máčajová, M., Meta, M., Čavarga, I., Bilčík, B., 2021. Chorioallantoic membrane models of various avian species: differences and applications. Biology (Basel). 10, 301. https://doi.org/10.3390/biology10040301.

Kurantowicz, N., Sawosz, E., Halik, G., Strojny, B., Hotowy, A., Grodzik, M., Piast, R., Pasanphan, W., Chwalibog, A., 2017. Toxicity studies of six types of carbon nanoparticles in a chicken-embryo model. Int. J. Nanomedicine 12, 2887–2898. https://doi.org/10.2147/IJN.S131960.

Lagarto, A., Vega, R., Guerra, I., González, R., 2006. *In vitro* quantitative determination of ophthalmic irritancy by the chorioallantoic membrane test with trypan blue staining as alternative to eye irritation test. Toxicol. in Vitro 20, 699–702. https://doi.org/10.1016/j.tiv.2005.10.003.

Leonard, R.C.F., Williams, S., Tulpule, A., Levine, A.M., Oliveros, S., 2009. Improving the therapeutic index of anthracycline chemotherapy: focus on liposomal doxorubicin (Myocet™). Breast. 18, 218–224. https://doi.org/10.1016/j.breast.2009.05.004.

Liu, M., Scanlon, C.S., Banerjee, R., Russo, N., Inglehart, R.C., Willis, A.L., Weiss, S.J., D'Silva, N.J., 2013. The histone methyltransferase EZH2 mediates tumor progression on the chick chorioallantoic membrane assay, a novel model of head and neck squamous cell carcinoma. Transl. Oncol. 6, 273–281. https://doi.org/10.1593/tlo.13175.

Liu, K., Holz, J.A., Ding, Y., Liu, X., Zhang, Y., Tu, L., Kong, X., Priem, B., Nadort, A., Lambrechts, S.A.G., Aalders, M.C.G., Buma, W.J., Liu, Y., Zhang, H., 2015. Targeted labeling of an early-stage tumor spheroid in a chorioallantoic membrane model with upconversion nanoparticles. Nanoscale. 7, 1596–1600. https://doi.org/10.1039/C4NR05638H.

Liu, P., Chen, G., Zhang, J., 2022. A review of liposomes as a drug delivery system: current status of approved products, regulatory environments, and future perspectives. Molecules. 27, 1372. https://doi.org/10.3390/molecules27041372.

Lokman, N.A., Elder, A.S.F., Ricciardelli, C., Oehler, M.K., 2012. Chick chorioallantoic membrane (CAM) assay as an *in vivo* model to study the effect of newly identified molecules on ovarian cancer invasion and metastasis. Int. J. Mol. Sci. 13, 9959–9970. https://doi.org/10.3390/ijms13089959.

McKenzie, B., Kay, G., Matthews, K.H., Knott, R.M., Cairns, D., 2015. The hen's egg chorioallantoic membrane (HET-CAM) test to predict the ophthalmic irritation potential of a cysteamine-containing gel: quantification using Photoshop® and ImageJ. Int. J. Pharm. 490, 1–8. https://doi.org/10.1016/j.ijpharm.2015.05.023.

Menegola, E., Broccia, M.L., Renzo, F.D., 2001. Teratogenic effects of doxorubicin in rats at midgestation and at term. Teratog. Carcinog. Mutagen. 21, 283–293. https://doi.org/10.1002/tcm.1016.

Moreno-Jiménez, I., Kanczler, J.M., Hulsart-Billstrom, G., Inglis, S., Oreffo, R.O.C., 2017. The chorioallantoic membrane assay for biomaterial testing in tissue engineering: a short-term *in vivo* preclinical model. Tissue Eng. Part C Methods. 23, 938–952. https://doi.org/10.1089/ten.TEC.2017.0186.

Munnier, E., Tewes, F., Cohen-Jonathan, S., Linassier, C., Douziech-Eyrolles, L., Marchais, H., Soucé, M., Hervé, K., Dubois, P., Chourpa, I., 2007. On the interaction of doxorubicin with oleate ions: fluorescence spectroscopy and liquid-liquid extraction study. Chem. Pharm. Bull (Tokyo). 55, 1006–1010. https://doi.org/10.1248/cpb.55.1006.

Murdan, S., Gregoriadis, G., Florence, A.T., 1999. Novel sorbitan monostearate organogels. J. Pharm. Sci. 88, 608–614. https://doi.org/10.1021/js980342r.

Murphy, J.B., 1914. Studies in tissue specificity: II. The ultimate fate of Mammalian tissue implanted in the chick embryo. J. Exp. Med. 19, 181–186. https://doi.org/10.1084/jem.19.2.181.

Nazaktabar, A., Lashkenari, M.S., Araghi, A., Ghorbani, M., Golshahi, H., 2017. *In vivo* evaluation of toxicity and antiviral activity of polyrhodanine nanoparticles by using the chicken embryo model. Int. J. Biol. Macromol. 103, 379–384. https://doi.org/10.1016/j.ijbiomac.2017.05.069.

Nowak-Sliwinska, P., Segura, T., Iruela-Arispe, M.L., 2014. The chicken chorioallantoic membrane model in biology, medicine and bioengineering. Angiogenesis. 17, 779–804. https://doi.org/10.1007/s10456-014-9440-7.

Palmeira-de-Oliveira, R., Machado, R.M., Martinez-de-Oliveira, J., Palmeira-de-Oliveira, A., 2018. Testing vaginal irritation with the Hen's Egg Test-Chorioallantoic Membrane assay. ALTEX 35, 495–503. https://doi.org/10.14573/altex.1710091.

Patel, S., Jana, S., Chetty, R., Thakore, S., Singh, M., Devkar, R., 2019. Toxicity evaluation of magnetic iron oxide nanoparticles reveals neuronal loss in chicken embryo. Drug Chem. Toxicol. 42, 1–8. https://doi.org/10.1080/01480545.2017.1413110.

Perez, A.T., Domenech, G.H., Frankel, C., Vogel, C.L., 2002. Pegylated liposomal doxorubicin (Doxil) for metastatic breast cancer: the Cancer Research Network, Inc., experience. Cancer Investig. 20, 22–29. https://doi.org/10.1081/cnv-120014883.

Poletto, F.S., Oliveira, C.P., Wender, H., Regent, D., Donida, B., Teixeira, S.R., Guterres, S.S., Rossi-Bergmann, B., Pohlmann, A.R., 2015. How sorbitan monostearate can increase drug-loading capacity of lipid-core polymeric nanocapsules. J. Nanosci. Nanotechnol. 15, 827–837. https://doi.org/10.1166/jnn.2015.9182.

Predoi, M.C., Mîndrilă, I., Buteică, S.A., Purcaru, Ş.O., Mihaiescu, D.E., Mărginean, O.M., 2020. Iron oxide/salicylic acid nanoparticles as potential therapy for B16F10 melanoma transplanted on the chick chorioallantoic membrane. Processes. 8, 706. https://doi.org/10.3390/pr8060706.

Rampino, A., Borgogna, M., Blasi, P., Bellich, B., Cesàro, A., 2013. Chitosan nanoparticles: preparation, size evolution and stability. Int. J. Pharm. 455, 219–228. https://doi.org/10.1016/j.ijpharm.2013.07.034.

Rampino, A., Borgogna, M., Bellich, B., Blasi, P., Virgilio, F., Cesàro, A., 2016. Chitosan-pectin hybrid nanoparticles prepared by coating and blending techniques. Eur. J. Pharm. Sci. 84, 37–45. https://doi.org/10.1016/j.ejps.2016.01.004.

Ribatti, D., 2017. The chick embryo chorioallantoic membrane (CAM) assay. Reprod. Toxicol. 70, 97–101. https://doi.org/10.1016/j.reprotox.2016.11.004.

Ribatti, D., Tamma, R., 2018. The chick embryo chorioallantoic membrane as an *in vivo* experimental model to study human neuroblastoma. J. Cell. Physiol. 234, 152–157. https://doi.org/10.1002/jcp.26773.

Roman, D., Yasmeen, A., Mireuta, M., Stiharu, I., Moustafa, A.-E.A., 2013. Significant toxic role for single-walled carbon nanotubes during normal embryogenesis. Nanomedicine. 9, 945–950. https://doi.org/10.1016/j.nano.2013.03.010.

Russell, W.M.S., Burch, R.L., 1959. The Principles of Humane Experimental Technique, London, Methuen. https://doi.org/10.5694/j.1326-5377.1960.tb73127.x.

Sahoo, S., Kumar, N., Bhattacharya, C., Sagiri, S.S., Jain, K., Pal, K., Ray, S.S., Nayak, B., 2011. Organogels: properties and applications in drug delivery. Des. Monomers Polym. 14, 95–108. https://doi.org/10.1163/138577211X555721.

Schomann, T., Qunneis, F., Widera, D., Kaltschmidt, C., Kaltschmidt, B., 2013. Improved method for *ex ovo*-cultivation of developing chicken embryos for human stem cell xenografts. Stem Cells Int. 2013, 960958 https://doi.org/10.1155/2013/960958.

Schütz, C.A., Juillerat-Jeanneret, L., Mueller, H., Lynch, I., Riediker, M., NanoImpactNet Consortium, 2013. Therapeutic nanoparticles in clinics and under clinical evaluation. Nanomedicine (London) 8, 449–467. https://doi.org/10.2217/nnm.13.8.

Sesarman, A., Muntean, D., Abrudan, B., Tefas, L., Sylvester, B., Licarete, E., Rauca, V., Luput, L., Patras, L., Banciu, M., Vlase, L., Porfire, A., 2021. Improved pharmacokinetics and reduced side effects of doxorubicin therapy by liposomal co-encapsulation with curcumin. J. Liposome Res. 31, 1–10. https://doi.org/10.1080/08982104.2019.1682604.

Shingadia, H.U., 2015. Hepatoprotective effects of herbal drug on Adriamycin induced toxicity in developing chick embryos. Am. J. Adv. Drug. Deliv. 3, 236–247.

Sousa, G.D., Kishishita, J., Aquino, K.A.S., Presgrave, O.A.F., Leal, L.B., Santana, D.P., 2017. Biopharmaceutical assessment and irritation potential of microemulsions and conventional systems containing oil from *Syagrus cearensis* for topical delivery of Amphotericin B using alternative methods. AAPS PharmSciTech 18, 1833–1842. https://doi.org/10.1208/s12249-016-0663-3.

Toley, B.J., Lovatt, Z.G.T., Harrington, J.L., Forbes, N.S., 2013. Microfluidic technique to measure intratumoral transport and calculate drug efficacy shows that binding is essential for doxorubicin and release hampers Doxil. Integr. Biol. 5, 1184–1196. https://doi.org/10.1039/c3ib40021b.

Tulubas, F., Gurel, A., Oran, M., Topcu, B., Caglar, V., Uygur, E., 2015. The protective effects of ω-3 fatty acids on doxorubicin-induced hepatotoxicity and nephrotoxicity in rats. Toxicol. Ind. Health 31, 638–644. https://doi.org/10.1177/0748233713483203.

Victorelli, F.D., Cardoso, V.M.O., Ferreira, N.N., Calixto, G.M.F., Fontana, C.R., Baltazar, F., Gremião, M.P.D., Chorilli, M., 2020. Chick embryo chorioallantoic membrane as a suitable *in vivo* model to evaluate drug delivery systems for cancer treatment: a review. Eur. J. Pharm. Biopharm. 153, 273–284. https://doi.org/10.1016/j.ejpb.2020.06.010.

Vu, B.T., Shahin, S.A., Croissant, J., Fatieiev, Y., Matsumoto, K., Doan, T.L.-H., Yik, T., Simargi, S., Conteras, A., Ratliff, L., Jimenez, C.M., Raehm, L., Khashab, N., Durand, J.-O., Glackin, C., Tamanoi, F., 2018. Chick chorioallantoic membrane assay as an *in vivo* model to study the effect of nanoparticle-based anticancer drugs in ovarian cancer. Sci. Rep. 8, 8524. https://doi.org/10.1038/s41598-018-25573-8.

Wilczewska, A.Z., Niemirowicz, K., Markiewicz, K.H., Car, H., 2012. Nanoparticles as drug delivery system. Pharmacol. Rep. 64, 1020–1037. https://doi.org/10.1016/s1734-1140(12)70901-5.

Zhao, Y., Alakhova, D.Y., Kim, J.O., Bronich, T.K., Kabanov, A.V., 2013. A simple way to enhance Doxil(R) therapy: drug release from liposomes at the tumor site by

amphiphilic block copolymer. J. Control. Release 168, 61–69. https://doi.org/10.1016/j.jconrel.2013.02.026.